Theoretical Insights into Ion Transport Mechanisms in Fluoroacetonitrile-Based Electrolytes for Li/Na/K Ion Batteries: A Molecular Dynamics and Quantum Chemical Study

Hang Liu[ab], Yi Huang[a], Siquan Li[b], Juan Yang[b], Pengjun Ma[b], Xu Zhang[b], Anmin Liu[c], Cuiying Lu[d], Peiyu Wang[a]*, Bingjun Yang[b*], Xingbin Yan[e]

[a]College of Electric Engineering, Key Laboratory for Electronic Materials of Northwest Minzu University, Gansu Engineering Research Center of Ecological Environment Intelligent Networking. Northwest Minzu University, Lanzhou, Gansu 730030, PR China

[b]Key Laboratory of Energy Conservation and Energy Storage Materials of Gansu Province, Research Center for Resource Chemistry and Energy Materials，State Key Laboratory of Solid Lubrication, Lanzhou Institute of Chemical Physics, Chinese Academy of Sciences, Lanzhou 730000, China

[c]School of Chemical Engineering, Ocean and Life Sciences, Dalian University of Technology, Panjin 124221, China.

[d]School of Chemistry and Chemical Engineering, Yulin University, Yulin 718500, China

[e]School of Materials Science and Engineering, Sun Yat-Sen University, Guangzhou 510275, China

*Corresponding author: yangbj@licp.cas.cn(B.J.Yang); wangpy03@126.com (P.Y.Wang);

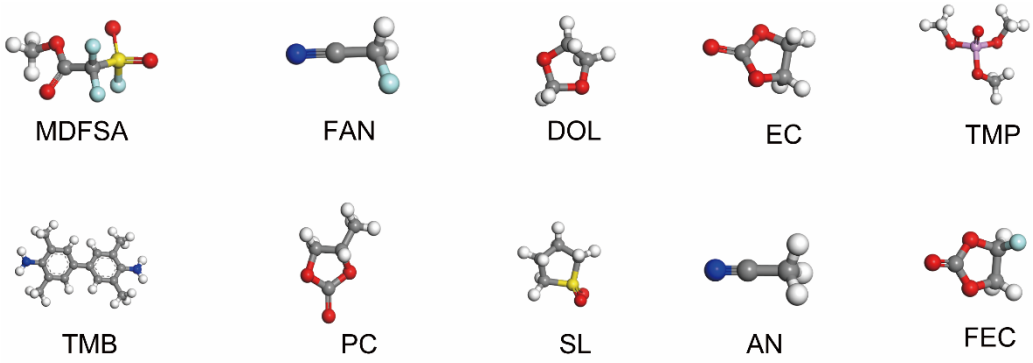

Figure S1. Solvent molecular models.

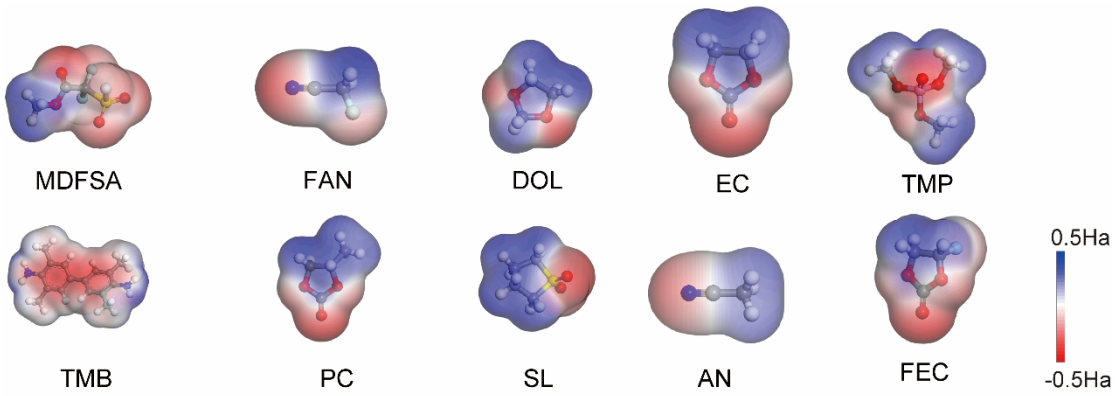

Figure S2. Electrostatic potential of solvent molecules

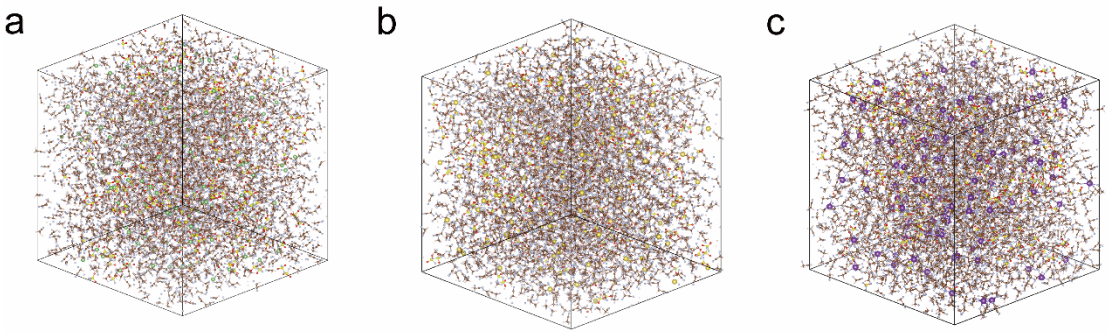

Figure S3. Snapshots of the molecular dynamics (MD) simulation of (a) LiFSI/FAN (b) NaFSI/FAN and (c) KFSI/FAN.

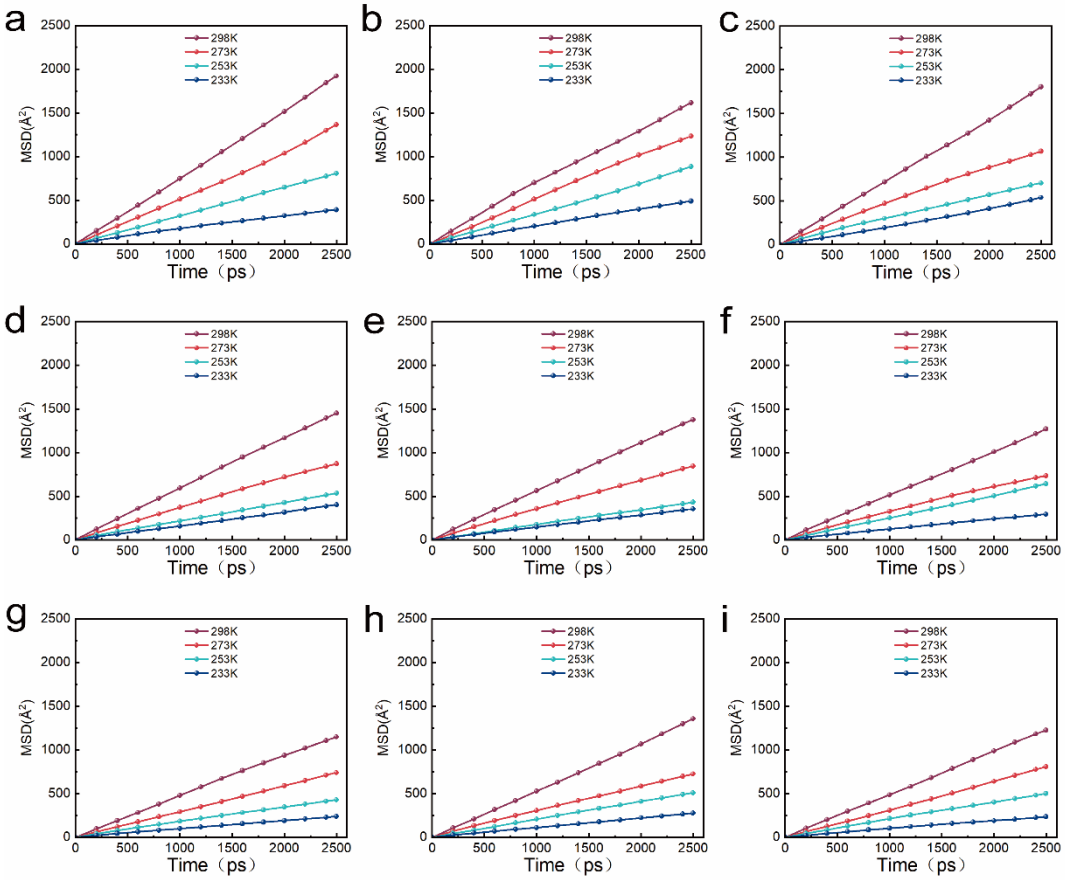

Figure S4. Mean squared displacement (MSD) of Li^+, Na^+ and K^+ ions from MD simulations of the electrolytes at various temperatures. (a-c) MSD plots for (a) Li^+, (b) Na^+ and (c) K^+ ions at a concentration of 0.5 M. (d-f) MSD plots for (d) Li^+, (e) Na^+ and (f) K^+ ions at a concentration of 2 M. (g-i) MSD plots for (g) Li^+, (h) Na^+ and (i) K^+ ions at a concentration of 3 M.

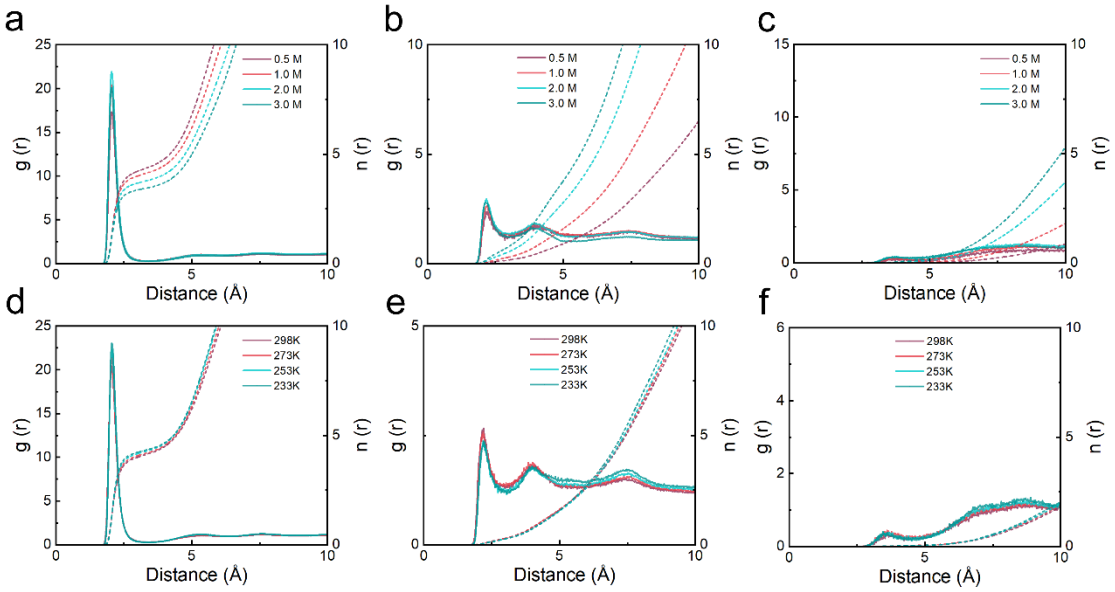

Figure S5. Radial distribution functions and coordination numbers of Li^+ with (a) N atoms, (b) O atoms, and (c) Li^+ in LiFSI/FAN electrolytes at 298 K and various concentrations; radial distribution functions and coordination numbers of Li^+ with (a) N atoms, (b) O atoms, and (c) Li^+ in LiFSI/FAN electrolytes at 1 M concentration and various temperatures.

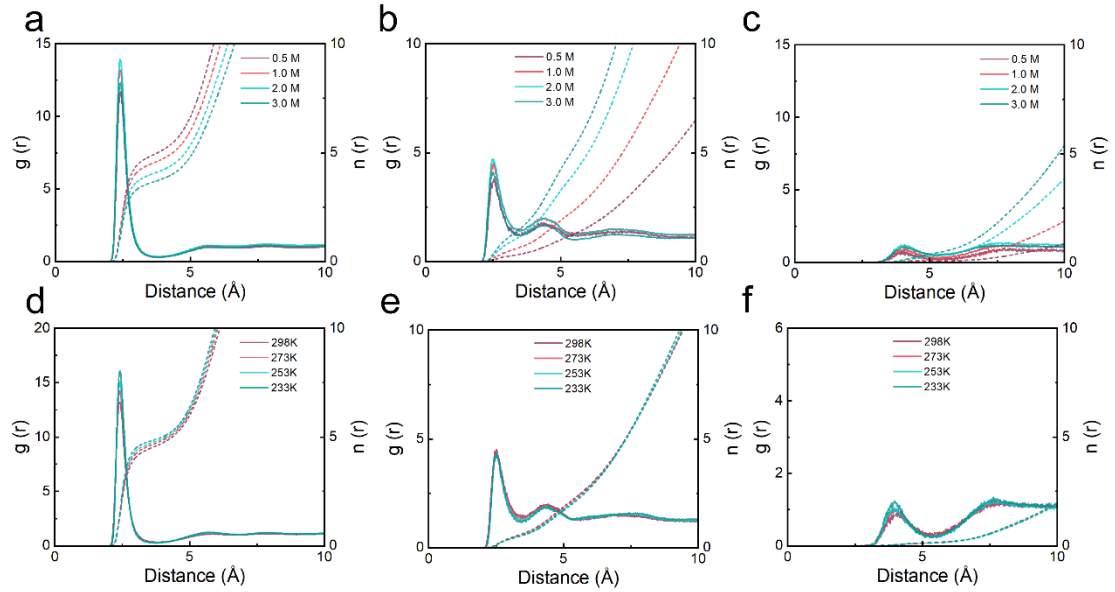

Figure S6. Radial distribution functions and coordination numbers of Na^+ with (a) N atoms, (b) O atoms, and (c) Na^+ in NaFSI/FAN electrolytes at 298 K and various concentrations; radial distribution functions and coordination numbers of Na^+ with (a) N atoms, (b) O atoms, and (c) Na^+

in NaFSI/FAN electrolytes at 1 M concentration and various temperatures.

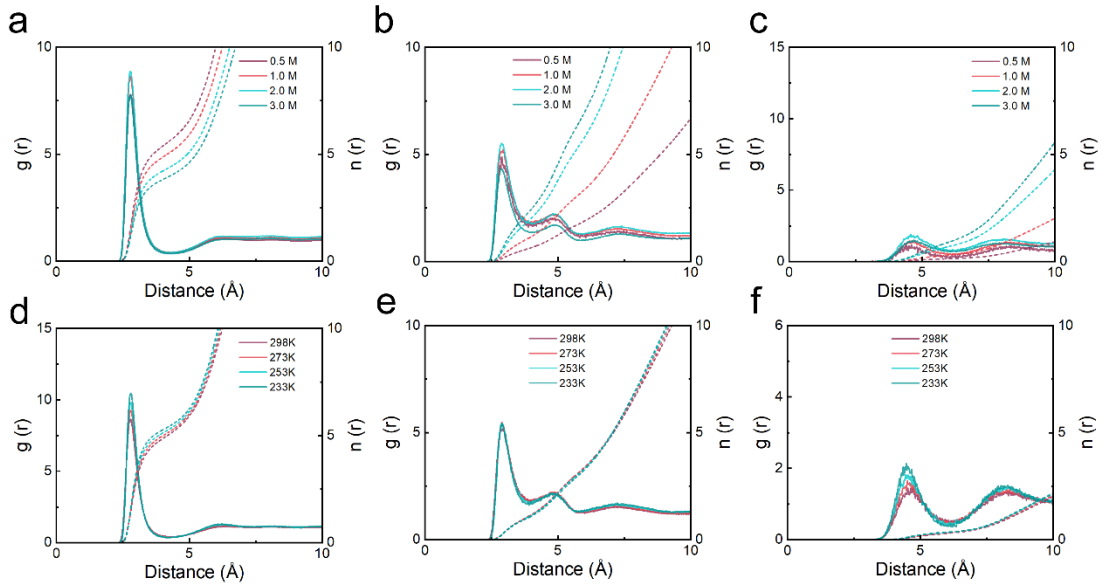

Figure S7. Radial distribution functions and coordination numbers of K^+ with (a) N atoms, (b) O atoms, and (c) K^+ in KFSI/FAN electrolytes at 298 K and various concentrations; radial distribution functions and coordination numbers of K^+ with (a) N atoms, (b) O atoms, and (c) K^+ in KFSI/FAN electrolytes at 1 M concentration and various temperatures.

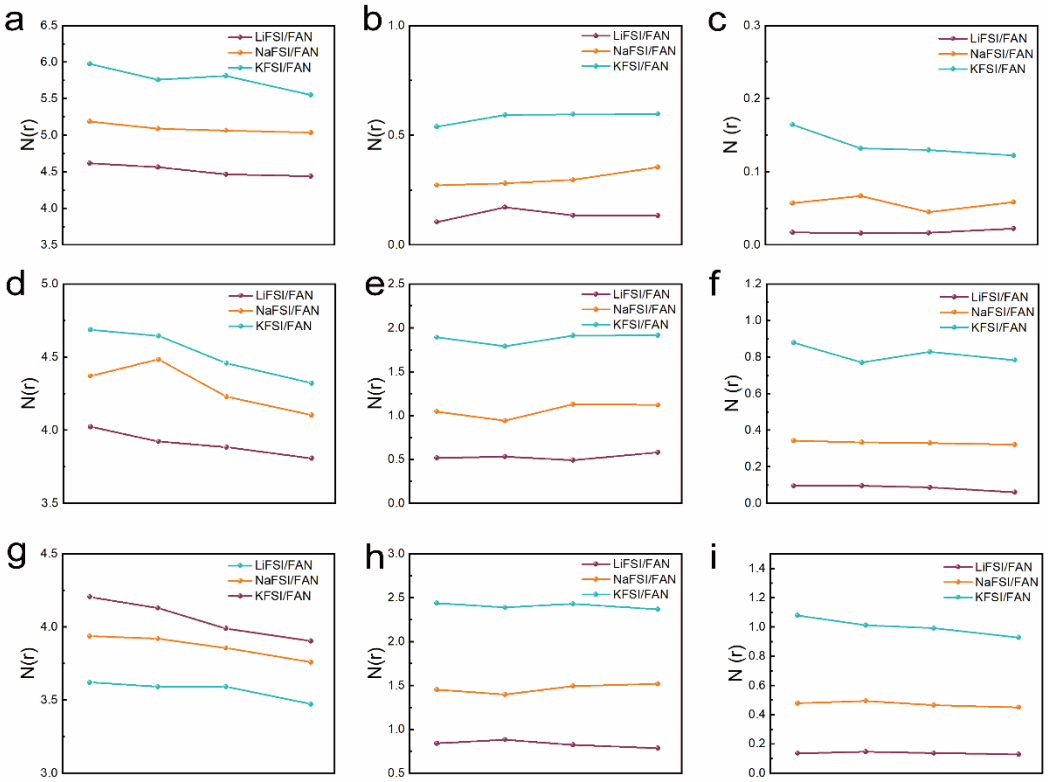

Figure S8. Coordination numbers (CN) of Li^+, Na^+ and K^+ ions with the nitrogen (N) atom of the FAN solvent and oxygen (O) atoms of the FSI^- anion. (a-c) CN as a function of temperature at 0.5 M: (a) Li^+, (b) Na^+ and (c) K^+. (d-f) CN as a function of temperature at 2 M: (d) Li^+, (e) Na^+ and (f) K^+. (g-i) CN as a function of temperature at 3 M: (g) Li^+, (h) Na^+ and (i) K^+.

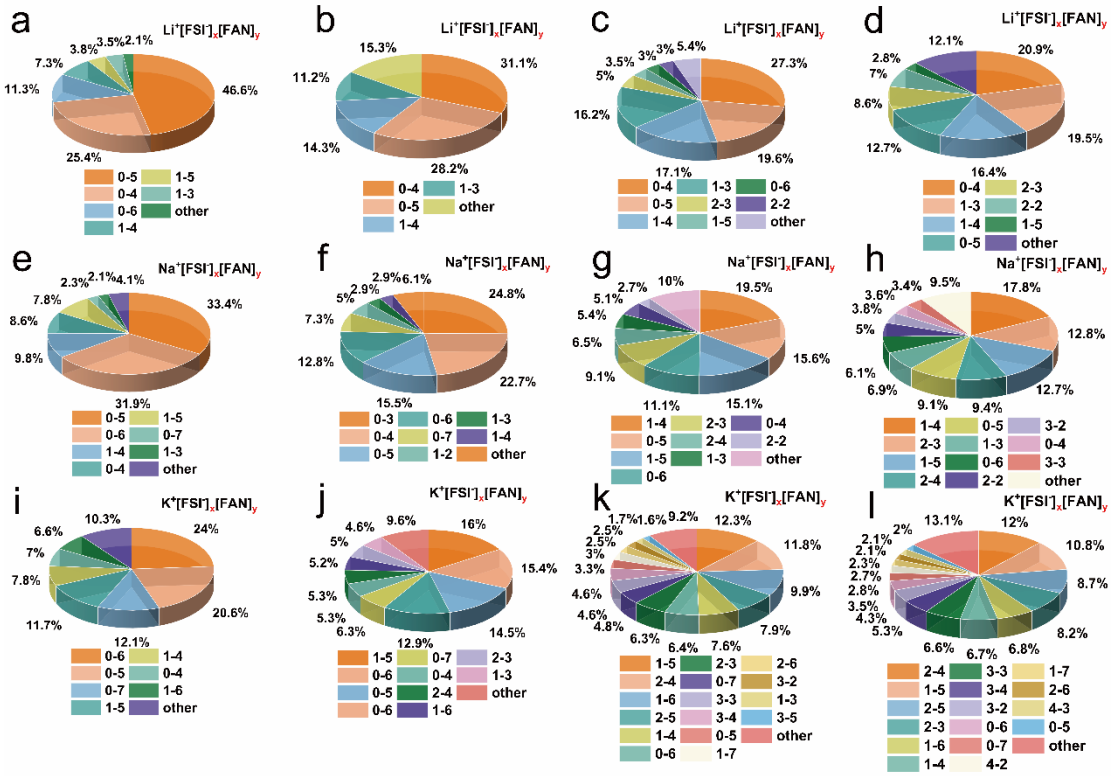

Figure S9. Analysis of the first solvation shell of Li^+ in LiFSI/FAN electrolytes at concentrations of (a) 0.5 M, (b) 1 M, (c) 2 M, and (d) 3 M (233 K). (e-h) First solvation shell structure of Na^+ in NaFSI/FAN electrolytes at corresponding concentrations of (e) 0.5 M, (f) 1 M, (g) 2 M, and (h) 3 M (233 K). (i-l) First solvation shell structure of K^+ in KFSI/FAN electrolytes at corresponding concentrations of 0.5 M, 1 M, 2 M, and 3 M (233 K).

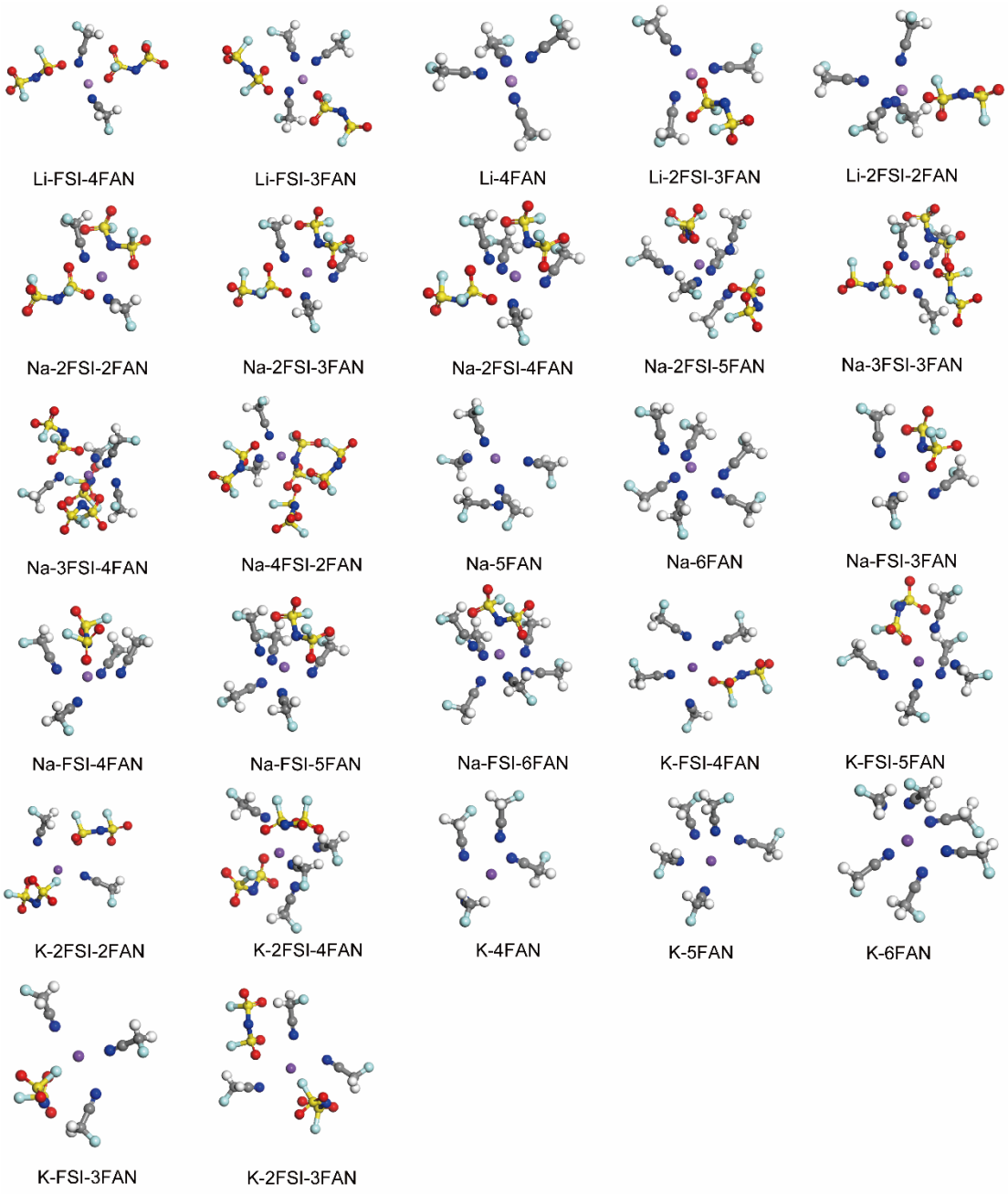

Figure S10. Solvation structures in the three FAN-based electrolytes containing different alkali metal ions (Li^+, Na^+, K^+).

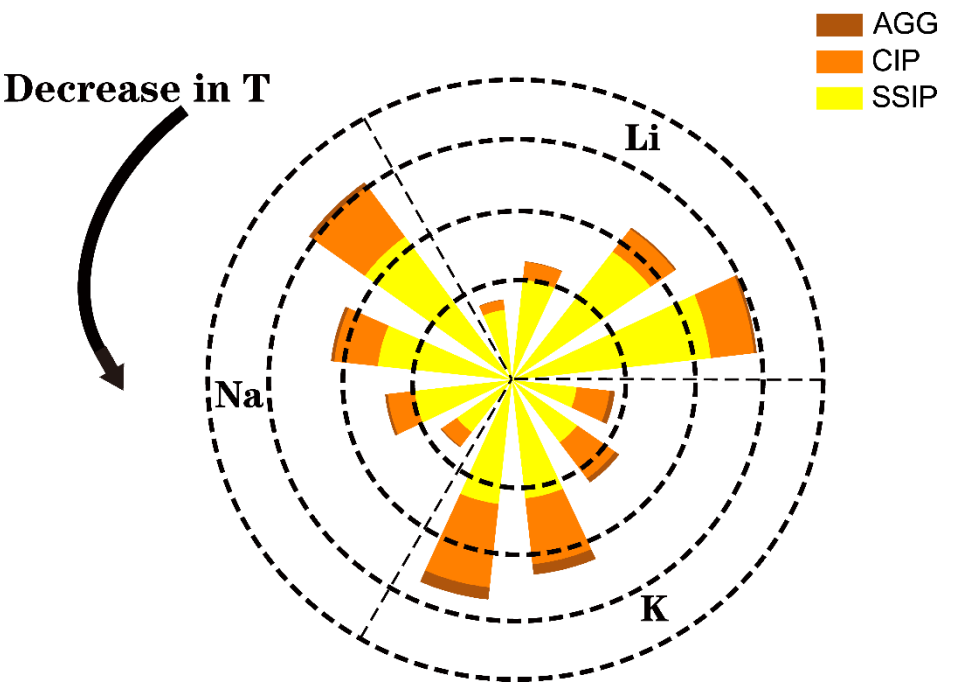

Figure S11. Ionic conductivity as a function of electrolyte composition at a concentration of 0.5 M. (The column heights represent the magnitude of ionic conductivity).

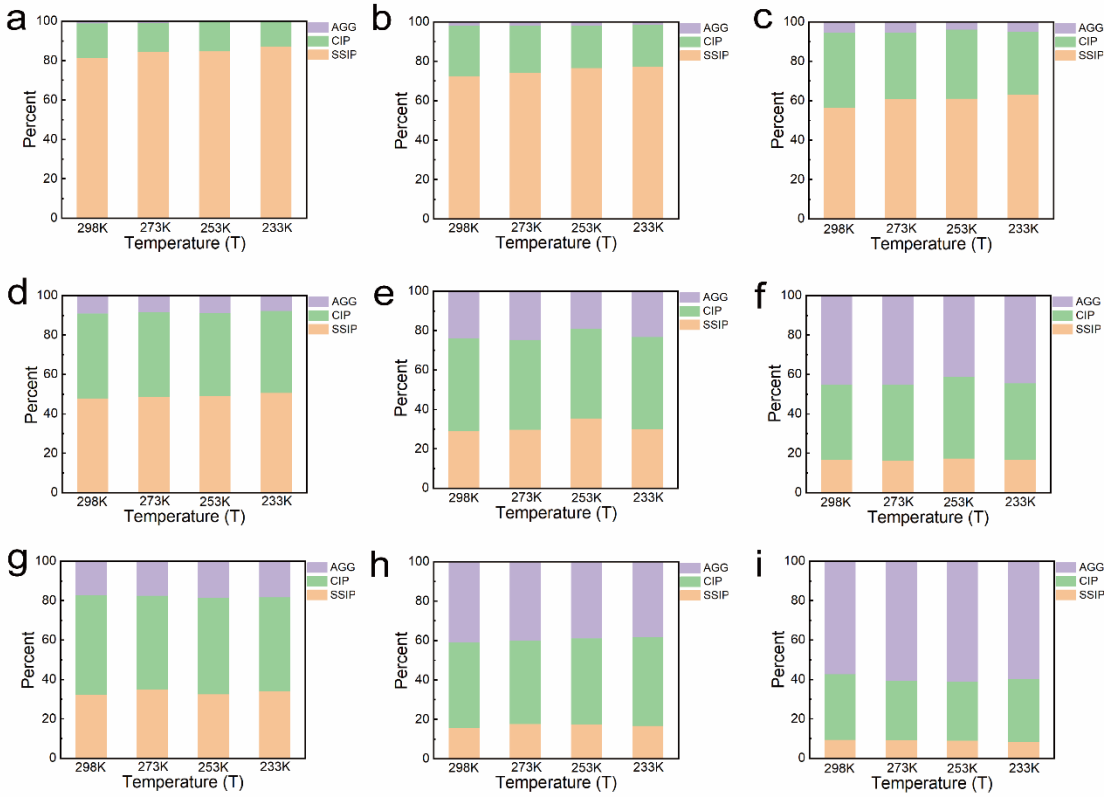

Figure S12. Proportion of various solvation structures as a function of temperature.(a-c) Proportions in the 0.5 M electrolyte, (d-f) Proportions in the 2 M electrolyte and (g-i) Proportions in the 3 M

electrolyte.

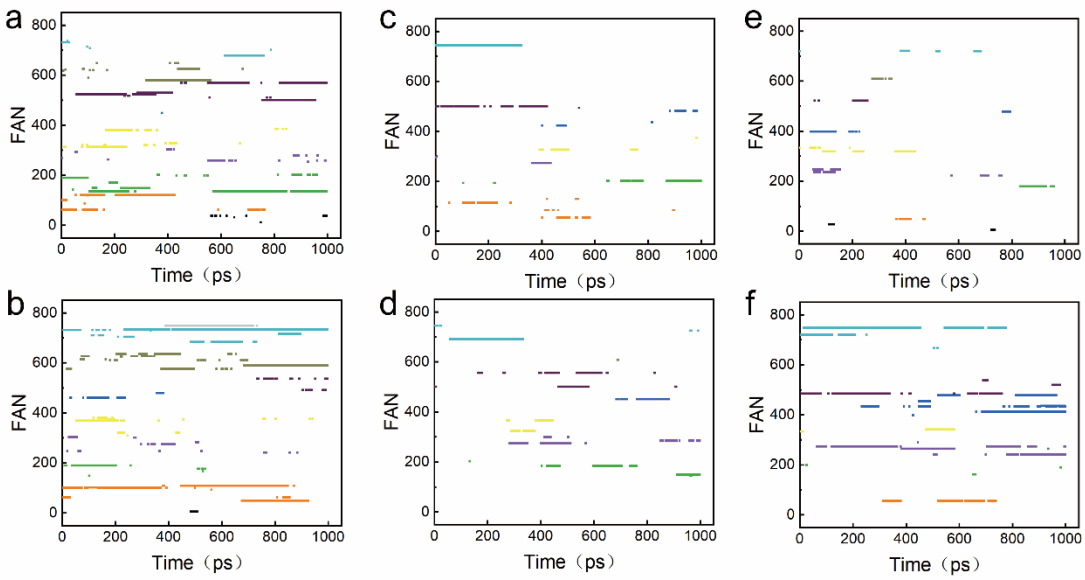

Figure S13. The vertical axis represents the index of solvent molecules coordinating to the central ion throughout the 1000 ps simulation. Horizontal bars indicate the residence time of N (from FAN) within the 3.0 Å cutoff distance of the ion. (a-c) Evolution of the solvation environments around alkali metal ions in 3 M electrolytes at 298 K:(a) Li^+, (b) Na^+ and (c) K^+. (d-f) Corresponding evolution at 233 K: (d) Li^+, (e) Na^+ and (f) K^+.

Table S1 Detailed composition of the LiFSI/FAN electrolyte at four different concentrations

System	Li^+	FSI^-	FAN
0.5 M LiFSIFAN	50	50	1797
1.0 M LiFSIFAN	125	125	2246
2.0 M LiFSIFAN	125	125	1123
3.0 M LiFSIFAN	125	125	749

Table S2 Detailed composition of the NaFSI/FAN electrolyte at four different concentrations

System	Na^+	FSI^-	FAN
0.5 M NaFSIFAN	50	50	1797
1.0 M NaFSIFAN	125	125	2246
2.0 M NaFSIFAN	125	125	1123
3.0 M NaFSIFAN	125	125	749

Table S3 Detailed composition of the KFSI/FAN electrolyte at four different concentrations

System	K^+	FSI^-	FAN
0.5 M KFSIFAN	50	50	1797
1.0 M KFSIFAN	125	125	2246
2.0 M KFSIFAN	125	125	1123
3.0 M KFSIFAN	125	125	749

Table S4 IUPAC Names and sizes of the solvent molecules used

Abbreviations	Name	Shell volume ($Å^3$)
MDFBA	Methyl2,2-difluoro-2(fluorosulfonyl)acetate	439.87 $Å^3$
FAN	Fluoroacetonitrile	119.19 $Å^3$
DOL	1,3-Dioxolane	168.53 $Å^3$
EC	Ethylene carbonate	166.28 $Å^3$
TMP	Trimethyl phosphate	343.33 $Å^3$
TMB	Trimethyl borate	674.31 $Å^3$
PC	Propylene carbonate	263.11 $Å^3$

SL	Sulfolane	265.13 Å^3
AN	Acetonitrile	101.27 Å^3
FEC	Fluoroethylene carbonate	179.37 Å^3